Table IX. Selected Distances and Angles Involving Nonbonded Atoms[a]

(a) Distances, Å

Te···C(12)	2.945 (9)	Te···Br(2′)	3.713 (1)

(b) Angles, deg

Br(1)-Te···C(12)	89.0 (2)	Br(1)-Te···Br(2′)	103.37 (4)
Br(2)-Te···C(12)	91.6 (2)	Br(2)-Te···Br(2′)	78.13 (4)
Br(3)-Te···C(12)	168.6 (2)	Br(3)-Te···Br(2′)	108.85 (4)
C(1)-Te···C(12)	71.5 (3)	C(1)-Te···Br(2′)	151.0 (2)
Br(2′)-Te···C(12)	82.4 (3)	Te′-Br(2′)···Te	101.87 (4)

[a] Unprimed atoms are in the symmetry position, x, y, z; primed atoms are in $1-x, 1-y, -z$.

are shown in Figure 2. The conversion of the trihalide to the dibenzotellurophene dihalide may be visualized as involving the formation of a bond between Te and C(12) as the Te–Br(3) and C(12)–H(12) bonds are broken. The biphenylyl moiety becomes planar in the process, but the remainder of the molecule, including the two axial halogens, is essentially unchanged.

The only intermolecular contacts in 2-biphenylyltellurium tribromide appreciably shorter than the sum of van der Waals radii are between Te and Br(2) at 3.713 (1) Å. (The sum of the van der Waals radii for these atoms is 4.15 Å.) These weak Te···Br(2′) and Te′···Br(2) interactions join pairs of molecules into loose dimers across centers of symmetry as indicated by dotted lines in Figure 1.

If one includes C(12) and Br(2′), the coordination about tellurium may be considered roughly octahedral, as depicted in Figure 2. The angles involved at tellurium in this extended description of the coordination are listed in Table IX.

Acknowledgment. The authors wish to thank Professor C. E. Strouse and Dr. Jane Strouse for help and advice on the use of the Syntex diffractometer. The financial help of the UCLA Academic Senate Committee on Research and the UCLA Campus Computing Network is also gratefully acknowledged.

Registry No. $C_{12}H_9TeBr_3$, 61288-79-7.

Supplementary Material Available: Table III, the calculated positions and assigned isotropic thermal parameters of the hydrogen atoms; Table IV, the root-mean-square amplitudes of vibration; and Table V, the observed and calculated structure factors (12 pages). Ordering information is given on any current masthead page.

References and Notes

(1) J. D. McCullough and C. Knobler, *Inorg. Chem.*, **15**, 2728 (1976).
(2) J. D. McCullough, *Inorg. Chem.*, **14**, 1142 (1975).
(3) J. D. McCullough, *Inorg. Chem.*, **12**, 2669 (1973), and references therein.
(4) G. D. Christofferson and J. D. McCullough, *Acta Crystallogr.*, **11**, 249 (1958).
(5) C. Knobler and J. D. McCullough, *Inorg. Chem.*, **11**, 3026 (1972).
(6) J. D. McCullough, *Inorg. Chem.*, **14**, 2285 (1975).
(7) P. Schulz and G. Klar, *Z. Naturforsch., B*, **30**, 43 (1975).
(8) The computer programs used in the present work are listed in footnote 4 of ref 2 above. The function $\sum w\|F_o| - |F_c\|^2$ was minimized in the least-squares refinement and the discrepancy indices were defined as $R = \sum\|F_o| - |F_c\|/\sum|F_o|$ and $R_w = [\sum w\|F_o| - |F_c\|^2/\sum w|F_o|^2]^{1/2}$, where $w = [1/\sigma(F_o)]^2$.
(9) In the SECEXT program, secondary extinction corrections are computed by use of the expression $F_{cor} = F_o(1 + C\beta J_o)^{1/2}$ with symbols defined by W. H. Zachariasen, *Acta Crystallogr.*, **16**, 1139 (1963). In the present case C has the value 6.7×10^{-6} and the maximum increase in a value of $|F|_{meas}$ is 43%.
(10) Supplementary materials.
(11) "International Tables for X-Ray Crystallography", Vol. IV, Kynoch Press, Birmingham, England, 1974.
(12) J. D. McCullough, *Inorg. Chem.*, **14**, 2639 (1975).

Contribution from the Department of Chemistry, University of Missouri, Columbia, Missouri 65201

Studies of the Ion *trans*-Dioxobis(ethylenediamine)osmium(VI). X-Ray Diffraction and Aqueous Oxygen-18 Exchange

JOHN M. MALIN,* E. O. SCHLEMPER, and R. KENT MURMANN

Received September 1, 1976 AIC60645H

The crystal structure of the *trans*-dioxobis(ethylenediamine)osmium(VI) bis(hydrogen sulfate) salt, $[Os(en)_2O_2](HSO_4)_2$, has been determined by x-ray diffraction techniques. Crystals of the compound belong to the monoclinic space group $P2_1/n$ with unit cell dimensions $a = 8.763$ (1) Å, $b = 14.697$ (3) Å, $c = 5.523$ (1) Å, and $\beta = 106.169$ (4)°. The density of 2.61 g/cm^3, calculated on the basis of two formula units per unit cell, agrees with the flotation density of 2.57 g/cm^3. Resolution of the structure was accomplished by Patterson and Fourier methods with refinement by full-matrix least-squares treatment leading to a conventional R factor of 5.84%. A total of 1205 independent reflections whose intensities were above background were used. Presence of an inversion center located on osmium dictates trans geometry for the $Os(en)_2O_2^{2+}$ ion. The osmium–oxygen distance is 1.74 ± 0.01 Å and the average osmium–nitrogen distance is 2.11 ± 0.01 Å. The intrachelate N–Os–N angle is 80.2 ± 0.5°. Strong hydrogen bonding between HSO_4^- ions in adjacent unit cells is observed (O---O = 2.56 (2) Å). Evidence is presented for weak hydrogen bonding involving HSO_4^- ions, osmyl oxygens, and amine moieties. The kinetics of exchange of oxygen atoms between the *trans*-dioxobis(ethylenediamine)osmium(VI) ion and solvent water has been investigated. Although decomposition of the complex precluded extensive measurements except at low temperature, the specific rate was found to increase with increasing pH in the range $1 \leq pH \leq 8.9$. At 0 °C and pH 4.3 the first-order specific rate of oxygen exchange is $2.9 \pm 0.1 \times 10^{-8}$ s^{-1}.

Introduction

Development of the aqueous chemistry of osmium has been limited by a scarcity of tractable starting materials.[1] Promising new routes to a variety of stable bis(ethylenediamine) osmium complexes are offered by the ion *trans*-dioxobis(ethylenediamine)osmium(VI) which is prepared in high yield from osmium tetroxide.[2,3] In this article we present an investigation of the ion employing x-ray diffraction techniques in the solid phase and oxygen-18-exchange measurements in aqueous solution.

Experimental Section

I. X-Ray Diffraction. Crystal Preparation. Crystals of $[Os(en)_2O_2]Cl_2$ were prepared as described previously[2,3] from osmium tetroxide (Englehard Industries, Inc.). Subsequently a 0.4-g sample of the salt was dissolved in ca. 20 ml of 0.5 M sulfuric acid and a column of cation-exchange resin (30 ml, Dowex 50X2-100) was

Table I. Atomic Positional Parameters[a]

	x	y	z
Os	0.0	0.0	0.0
S	−0.4679 (4)	0.2148 (3)	0.0642 (8)
O(1)	−0.1063 (12)	0.0285 (7)	0.2133 (18)
O(2)	−0.2987 (13)	0.2106 (9)	0.0187 (24)
O(3)	−0.4419 (17)	0.2394 (9)	0.3273 (24)
O(4)	0.4517 (14)	0.2870 (8)	−0.1064 (27)
O(5)	0.4596 (15)	0.1290 (8)	−0.0024 (24)
N(1)	0.1644 (14)	0.1037 (8)	0.1610 (25)
N(2)	−0.1637 (14)	0.0759 (8)	−0.2776 (22)
C(1)	−0.2673 (18)	0.0753 (10)	0.4069 (30)
C(2)	−0.3121 (18)	0.0238 (10)	−0.3878 (33)
H1C1	0.3618	0.1124	0.4547
H2C1	0.2122	0.0811	0.5355
H1C2	0.3679	−0.0476	0.5468
H2C2	0.3792	−0.0283	0.2734
H1N1	0.1110	0.1536	0.1806
H2N1	0.2224	0.1169	0.0593
H1N2	0.1211	−0.0905	0.4001
H2N2	0.1867	−0.1274	0.2104

[a] Standard deviations from the least-squares refinement are included in parentheses in this and other tables. Hydrogen atom parameters are calculated for chemically reasonable positions.

charged with the osmyl complex. The column was washed with several volumes of 0.05 M sulfuric acid until no chloride ion was present in the eluent, and the complex was eluted with 3 M H_2SO_4. While heating gently, the volume of this solution was reduced by rotary evaporation under vacuum until microcrystals began to form. At this point evaporation was terminated; the solution was warmed to redissolve the crystals and stored for several weeks in a refrigerator at ca. 5 °C. Single crystals of $[Os(en)_2O_2](HSO_4)_2$ formed slowly. These were collected on a sintered-glass filter, washed with methanol, and air-dried. Anal. Calcd for $OsO_{10}C_4N_4H_{18}S_2$: C, 8.95; H: 3.38; N, 10.44. Found: C, 8.84; H, 3.52; N, 10.38.

Data Collection. Preliminary precession and Weissenberg photographs of the yellow crystals indicated a monoclinic cell. The systematic absences (k odd for $0k0$ and $h + l$ odd for $h0l$) indicated the space group $P2_1/n$. A small, needlelike crystal was chosen for the intensity measurements because of the relatively high absorption correction (μ = 100.92). After shortening of the crystal with a razor blade the approximate dimensions were 0.06 × 0.10 × 0.34 mm. It was bounded by eight faces, all of low indices.

The crystal was mounted on a Picker four-circle diffractometer with the c axis nearly coincident with the ϕ axis of the instrument. Setting angles of 18 intense reflections were determined using Mo Kα radiation (λ 0.7107 Å). The cell constants determined by a least-squares refinement using these reflections were a = 8.763 (1) Å, b = 14.697 (3) Å, c = 5.523 (1) Å, and β = 106.169 (4)°.[5] The density calculated for 2 formula units per unit cell was 2.61 g/cm^3, in agreement with the observed density of 2.57 g/cm^3 obtained by flotation methods in a mixed-solvent system. A refinement using the 18 reflections was obtained to calculate the setting angles of all reflections measured. Intensities of 2773 reflections were measured up to a maximum 2θ angle of 40.0°. The count rate never exceeded 8000 counts/s and thus was in the linear region of the counter. Diffracted Mo Kα radiation was filtered through 1 mil of niobium foil in front of a 3 × 3 mm receiving aperture at a takeoff angle of 2.0°. A scan rate of 1.0°/min was used for the variable symmetric 2θ scan, taken from 0.40° below the 2θ setting for Kα_1 (λ 0.709 26 Å) to 0.40° above the 2θ setting for Kα_2 (0.713 54 Å). Stationary background counts of 20 s were recorded at both the high- and low-angle ends of the scan. Three reflections chosen as standards were measured after every 50 determinations. The averaged intensity of these three standards was found to increase linearly by 12% for the first 914 reflections and to decrease in stages by 25% over the final 1859 measurements. Since the color of the crystal changed to dark amber during this time, the decrease in intensity is ascribed to x-ray-induced decomposition of the compound. The initial growth in intensity may have resulted from an increase in the mosaic character of the crystal during the initial stages of decomposition. Corrections for these fluctuations were applied to the measured intensities. However, decomposition of the crystal undoubtedly presented the largest source of error in refining the structure.

Data Reduction. Counting statistical analysis and corrections for Lorentz–polarization were performed employing the usual equations. Crystal dimensions and facial indices were found by optical goniometric and microscopic techniques. The transmission correction factors ranged from 0.32 to 0.47. From the 2773 measured intensities, 1841 independent data points were obtained of which 1205 had intensities greater than 2θ, where $\sigma = [\sigma^2_{\text{counting}} + (0.035F_o^2)^2]^{1/2}$. These reflections were used in the structure determination.

Determination and Refinement of the Structure. Symmetry considerations placed the osmium atom on an inversion center. Most of the nonhydrogen atoms were located employing a three-dimensional Patterson synthesis. To locate the remaining nonhydrogen atoms a three-dimensional Fourier synthesis was used. The scattering factors applied to Os were those of Cromer and Waber[6a] while the anomalous scattering factors for that element were from Cromer.[6b] The N and C scattering factors were taken from Ibers[6c] and those of Stewart, Davidson, and Simpson[6d] were used for hydrogen. Anomalous scattering effects were included in F_c in the refinements. Least-squares refinement of positional and isotropic thermal parameters for all atoms except hydrogen converged with $R = \sum(||F_o|^2 - |kF_c|^2|/\sum|F_o|^2 = 0.169$ and $r = [\sum w(|F_o|^2 - |kF_c|^2)^2/\sum w(|F_o|)^4]^{1/2} = 0.236$, where $w = 1/\sigma^2(F_o^2)$ and k is a refinable scale factor. In this and all refinements the function $\sum w(F_o^2 - F_c^2)^2$ was minimized. Refinement with anisotropic temperature factors reduced R to 0.114 and r to 0.159. Inclusion of hydrogen atoms in chemically reasonable positions with isotropic temperature factors 1 Å^2 greater than those of the atoms to which they were attached gave R = 0.099 and r = 0.138. The standard deviation of an observation of unit weight was 2.29. The conventional agreement factor was 0.058. In the last cycle of refinement none of the atoms shifted by more than 0.1σ for a given parameter. The observed and calculated structure factors (×10) are available. All atom positions are given in Table I. The final thermal parameters of all nonhydrogen atoms are included in Table II.

II. Isotropic Exchange Experiments. Preparation of Reagents. Oxygen-18-enriched water was obtained from YEDA, Rehovot, Israel, and had an ^{18}O content of approximately 1.5 atom %. Samples of *trans*-dioxobis(ethylenediamine)osmium(VI) ion containing oxygen-18 were prepared by allowing the salt $[Os(en)_2O_2]Cl_2$ dissolved in enriched water to stand for 20 min at ca. 60 °C. The complex was precipitated from solution by adding an excess of cold saturated KCl solution. After about 15 min the solid ^{18}O-enriched salt was washed with absolute methanol and then with ether and dried in vacuo.

Reagent grade ethylenediamine was purified by slow distillation at atmospheric pressure. The first and last thirds of the distillate were

Table II. Atomic Anisotropic Thermal Parameters[a]

Atom	β_{11}	β_{22}	β_{33}	β_{12}	β_{13}	β_{23}
Os	0.0048 (1)	0.0017 (0)	0.0146 (3)	−0.0001 (1)	0.0052 (1)	0.0001 (1)
S	0.0061 (5)	0.0023 (2)	0.0224 (17)	−0.0000 (2)	0.0066 (7)	0.0000 (4)
O(1)	0.0088 (15)	0.0020 (4)	0.0082 (40)	−0.0017 (6)	0.0019 (20)	−0.0032 (10)
O(2)	0.0074 (15)	0.0050 (7)	0.0347 (56)	0.0013 (9)	0.0107 (25)	−0.0005 (16)
O(3)	0.0144 (23)	0.0054 (8)	0.0202 (50)	−0.0012 (10)	0.0071 (29)	−0.0038 (15)
O(4)	0.0076 (15)	0.0026 (5)	0.0462 (63)	0.0005 (8)	0.0057 (26)	0.0032 (16)
O(5)	0.0131 (22)	0.0024 (5)	0.0423 (63)	−0.0024 (8)	0.0142 (33)	−0.0035 (14)
N(1)	0.0049 (16)	0.0022 (5)	0.0199 (54)	−0.0018 (7)	0.0038 (24)	−0.0015 (14)
N(2)	0.0063 (17)	0.0025 (6)	0.0094 (48)	0.0014 (8)	0.0023 (24)	0.0003 (13)
C(1)	0.0075 (21)	0.0027 (7)	0.0150 (60)	0.0002 (10)	0.0051 (31)	0.0012 (16)
C(2)	0.0070 (19)	0.0018 (6)	0.0279 (71)	−0.0007 (8)	0.0093 (32)	−0.0006 (15)

[a] The anistropic thermal parameters are in the form $\exp[-(h^2\beta_{11}{}^2 + k^2\beta_{22}{}^2 + l^2\beta_{33}{}^2 + 2\beta_{12}hk + 2\beta_{13}hl + 2\beta_{23}kl)]$.

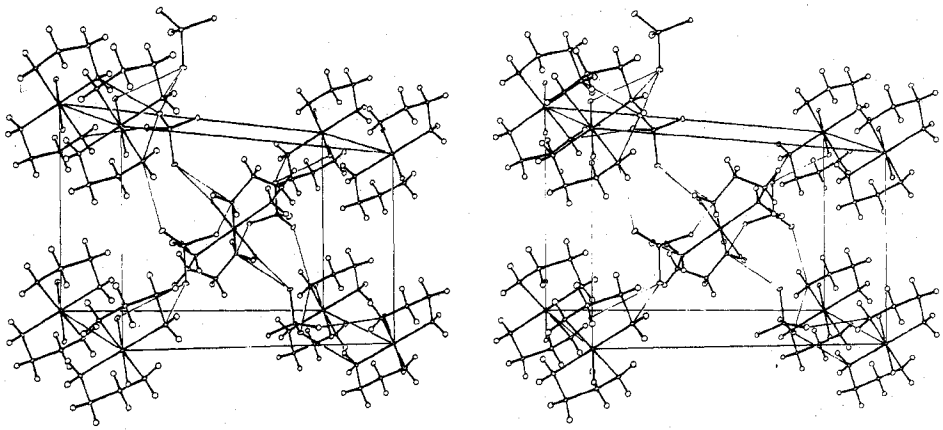

Figure 1. Stereoscopic view of the $[OsO_2(en)_2](HSO_4)_2$ unit cell. Light lines represent interionic hydrogen bonds.

Table III. Non-Hydrogen-Bonded Interionic Contacts (Å)

S-O(4)	3.62 (1)	O(3)-C(2)	3.58 (2)
O(1)-O(4)	2.88 (1)	O(3)-C(1)	3.62 (2)
O(1)-C(2)	3.21 (2)	O(3)-O(2)	3.64 (2)
O(1)-C(1)	3.22 (2)	O(3)-N(2)	3.67 (2)
O(1)-O(1)	3.30 (2)	O(3)-O(2)	3.70 (2)
O(2)-C(1)	3.29 (2)	O(4)-C(1)	3.41 (2)
O(2)-C(2)	3.53 (2)	O(5)-C(1)	3.32 (2)
O(2)-N(1)	3.33 (2)	O(5)-C(2)	3.59 (2)
O(3)-O(4)	3.38 (2)	O(5)-C(2)	3.64 (2)
O(3)-O(4)	3.57 (2)		

discarded and the middle fraction boiling at 116.5–117.0 °C was used. Anhydrous ethylenediamine dihydrochloride was produced by the reaction of the purified ethylenediamine in absolute methanol with gaseous HCl. Analysis of the vacuum-dried salt gave 52.90% Cl (calcd 53.38%). The water used in the experiments was doubly distilled, the second distillation being from acidic $K_2Cr_2O_7$ in an all-glass apparatus. Other substances were of reagent grade and were used without further purification.

$[Os(en)_2O_2]^{2+}$–H_2O Exchange. Exchange runs were initiated by adding approximately 0.4 mmol of oxygen-18-labeled *trans*-dioxobis(ethylenediamine)osmium(VI) ion to 50 ml of a solution containing the appropriate amounts of ethylenediamine dihydrochloride and HCl or NaOH at the desired temperature. Prior to addition, dry nitrogen gas was bubbled through the solution for at least 15 min. Subsequent to initiation, the reaction vessel was stoppered with a neoprene disk. At measured times after dissolution of the osmium salt, 5- or 10-ml samples of the solution were removed by syringe-transfer technique and cooled in a small test tube at 0 °C. The osmyl complex was precipitated quantitatively by addition of excess solid ammonium bromide. (Initial experiments using NaI showed more rapid precipitation but some nonreproducible, induced exchange.) As will be seen, the exchange rate is very low and thus the advantage of quick crystallization is unimportant. The precipitate, $[Os(en)_2O_2]Br_2$, was collected on a small sintered-glass filter, washed with a small amount of water at 0 °C and then acetone, and dried under a stream of dry nitrogen gas. After transfer to a break-seal tube, the sample was again dried for at least 12 h at 10^{-4} Torr.

By using a Nuclide RMS Isotopic Ratio mass spectrometer, samples were analyzed for oxygen-18 content employing a modification of the method of Anbar and Guttman,[7] which has been described by Kriege and Murmann.[8] The 46/(44 + 45) mass ratio of each unknown was compared with a "standard" CO_2 sample arbitrarily given the value 4.000×10^{-3} resulting in a normalized value of the ratio, R_N, for the sample. Since the enrichments were small, R_N is a satisfactory measure of the fractional ^{18}O content of the sample. Experimental data were plotted as graphs of $-\ln (R_N - R_{N\infty})$ vs. time. The slope (k_{obsd}) and intercept ($-\ln (R_{N_0} - R_{N\infty})$), were evaluated by the use of a weighted linear least-squares computer program utilizing an IBM 370/168 computer. In some instances plots were made of $-\ln (1 - F)$ vs. time. F is defined as the fraction of exchange completed.

Results and Discussion

Nature of the Crystal Structure. The structure consists of discrete *trans*-dioxobis(ethylenediamine)osmium(VI) complex cations and hydrogen sulfate anions (Figures 1 and 2). In Tables III and IV all nonhydrogen interionic distances under 3.7 Å are given. Except for the rather short separation between O(1) and O(4) (2.89 (1) Å), the shortest contacts are hydrogen bonds (Table IV) involving amine nitrogens, the osmyl oxygen, and the hydrogen sulfate ion. These hydrogen bonds stabilize the crystal structure.

The geometry of the hydrogen sulfate ion leaves no doubt that hydrogen is attached to O(2). The S–O(2) bond length

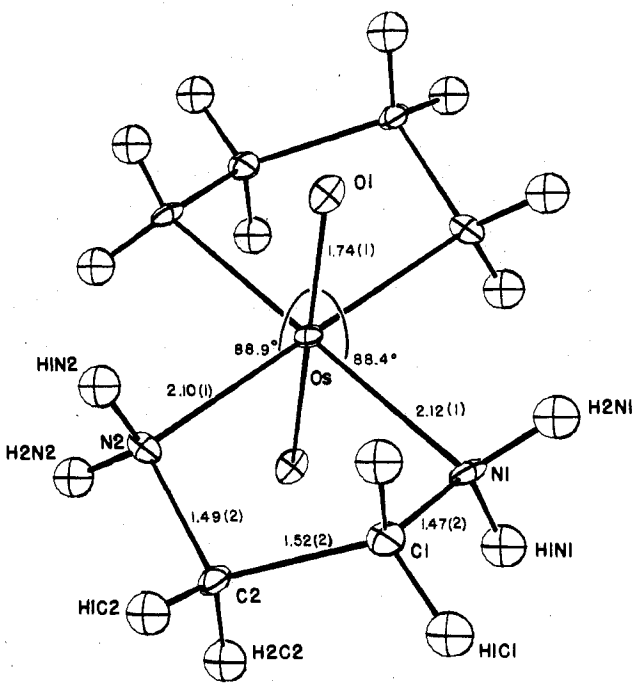

Figure 2. Perspective view of the *trans*-dioxobis(ethylenediamine)osmium(VI) complex ion showing bond distances.

Table IV. Hydrogen-Bonded Interionic Contacts

Atoms	H-bond dist, Å	S–O dist, Å
O(5)-N(1)	2.99 (2)	1.41 (1)
O(3)-N(1)	2.93 (2)	1.45 (1)
O(3)-N(2)	3.29 (2)	
O(4)-O(2)	2.56 (2)	1.46 (1)
O(4)-N(1)	3.00 (2)	
O(4)-N(2)	3.06 (2)	
O(2)-O(4)	2.56 (2)	1.57 (1)
O(2)-N(2)	3.01 (2)	
O(2)-O(1)	3.18 (2)	
O(1)-N(2)	3.07 (2)	

Table V. Intramolecular Bond Angles (deg)

O(1)-Os-N(2)	88.9 (5)	O(2)-S-O(5)	107.4 (7)
O(1)-Os-N(1)	88.4 (5)	O(2)-S-O(4)	103.3 (7)
N(1)-Os-N(2)′	99.8 (5)	O(2)-S-O(3)	106.1 (7)
N(1)-Os-N(2)	80.2 (5)	O(3)-S-O(5)	114.6 (8)
Os-N(2)-C(2)	111.5 (9)	O(3)-S-O(4)	112.1 (8)
Os-N(1)-C(1)	110.7 (9)	O(4)-S-O(5)	112.2 (8)
N(2)-C(2)-C(1)	108 (1)		
N(1)-C(1)-C(2)	108 (1)		

is 1.57 (1) Å while the S–O(3), S–O(4), and S–O(5) distances are 1.45 (1), 1.46 (1), and 1.41 (1) Å, respectively. Also, attachment of hydrogen to O(2) is supported by the O(2)–S–O(3), –O(4), and –O(5) angles which are all less than tetrahedral. The S–O(H) distance may be compared with known values of 1.56 (2) Å found in $KHSO_4$[9] and 1.61 (1) Å in $NaHSO_4 \cdot H_2O$.[10] Variations in the bond lengths S–O(3), S–O(4), and S–O(5) are greater than experimental error. As can be seen in Table IV, this may be ascribable to differences in hydrogen bonding among the oxygens. The shortest S–O distance (S–O(5), 1.41 (1) Å) is found for the sulfate oxygen that least participates in hydrogen bonding, having a single contact with N(1). The longer S–O distances are found for O(3) and O(4) which are involved in two and three hydrogen-bonding interactions, respectively. A short hydrogen bond (2.56 (2) Å) joins O(4) of hydrogen sulfate with O(2) in an adjacent unit cell.

Figure 2 shows that the ion $Os(en)_2O_2^{2+}$ has distorted octahedral geometry. A linear O=Os=O grouping is dictated by the inversion center at Os. The osmium–oxygen distance, 1.74 (1) Å, indicates a metal–oxygen double bond. The bond length can be compared with values of 1.710 (7), 1.75 (2), and 1.77 Å found, respectively, for OsO_4,[11] $K_2[OsO_2Cl_4]$,[12] and $K_2[OsO_2(OH)_4]$.[13] Although the osmyl oxygens participate in hydrogen bonding with HSO_4^-, the Os=O distance does not indicate protonation of the complex. Terminal osmium(VI)–oxygen triple bonds have been postulated for compounds in which the Os=O distance is ca. 1.67 Å.[14]

The osmium–oxygen axis is not precisely perpendicular to the plane of the four nitrogens but is inclined slightly, yielding O(1)–Os–N(1) and O(1)–Os–N(2) angles of 88.4 (5) and 88.9 (5)°, respectively. The plane about osmium is distorted toward rectangular rather than square geometry because of the limited span of the chelating ethylenediamine. Thus the interior angle N(1)–Os–N(2) is only 80.2 (5)° while the exterior N(1)–Os–N(2)′ angle is 99.8 (5)°. The average osmium–nitrogen distance is 2.11 (1) Å.

Both ethylenediamine ligands are in the gauche conformation. They exhibit bond distances and angles that are not significantly different from those commonly found in ethylenediamine chelates. Figure 2 contains the important bond distances for all atoms except hydrogen. Table V lists the important bond angles.

Aqueous Oxygen-18 Exchange. Aqueous Formula of the Ion $Os(en)_2O_2^{2+}$. The single-crystal x-ray diffraction study demonstrated that the ion $Os(en)_2O_2^{2+}$ has distorted octahedral geometry in the solid state with a linear O–Os–O grouping. The Os–O bonds have appreciable multiple-bond character. In the isotopic exchange work it was found that samples of oxygen-18-enriched $[Os(en)_2O_2^{2+}]$ can be dissolved in normal water and reprecipitated with less than 0.1% exchange. This establishes that the ion in aqueous solution retains the first coordination sphere of the solid. Reversible expansion to a coordination number of 7 or 8, if it occurs at all, must be quite slow.

$Os(en)_2O_2^{2+}$–H_2O Exchange. The initial ^{18}O-exchange experiments with aqueous $[Os(en)_2O_2]^{2+}$ showed the exchange to be slow in acidic solution (half-times of weeks) but to increase substantially when the pH was raised from 1.0 to 9. Also, especially at the higher pH values, some decomposition took place as evidenced by a darkening of the solution color, the presence of an OsO_4 odor, and deviation from linear first-order kinetics plots. It seemed likely that the decomposition reaction or its products were responsible for the apparent base catalysis of exchange. In order to decrease the effect of decomposition a lower temperature was used since the activation energy of the decomposition process was expected to be greater than that for exchange. A plot of $-\ln(1 - F)$ vs. time using data taken at 0 °C and pH 7.0 is shown in Figure 3 to be nearly linear for the first half-life, approximately 8 days. At the end of this period only slight discoloration could be seen. Even at 0 °C, k_{obsd} increases with pH and approximately follows $k_{obsd} = k[H^+]^{-1/2}$ with $k = 2.4 \pm 1 \times 10^{-10}$ $M^{1/2}$ s^{-1}. This equation has only qualitative significance mechanistically but is useful in predicting apparent rate constants.

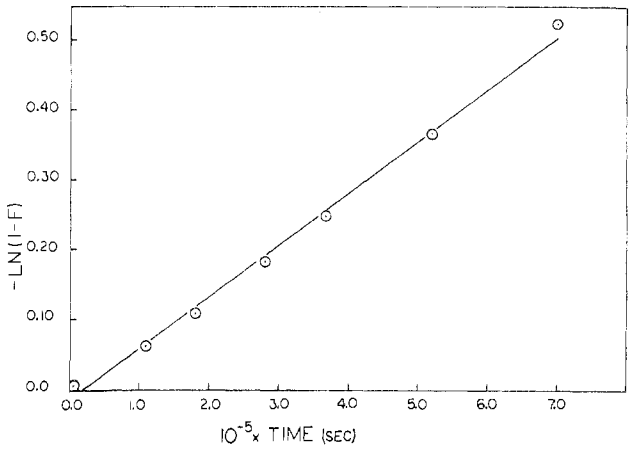

Figure 3. Plot of $-\ln(1 - F)$ vs. time at pH 7.0, 0 °C.

Table VI. Specific Rate of Oxygen-18 Exchange in Aqueous $[Os^{18}O_2(en)_2^{2+}]$[a]

Run	pH	Temp, °C	$[Os^{VI}]$, M	[en·2HCl], M	$10^8 k_{obsd}$, s^{-1}
1	2.0	0	0.0165	0	7.70 ± 1.7
2	4.3	0	0.0158	0.0040	2.90 ± 0.14
3	5.1	0	0.0148	0.0038	5.78 ± 0.19
4	6.14	0	0.0152	0.0038	13.3 ± 0.5
5	7.05	0	0.0172	0.0045	74.3 ± 2.3
6	7.45	0	0.0158	0.0038	189 ± 19
7	8.53	0	0.0183	0.0043	470 ± 58
8	9.3	0	0.0180	0.0054	1820 ± 110
9	1.0	25	0.01656	0.0186	46 ± 2.6
10	2.0	25	0.01675	0	24 ± 1.9
11	2	25	0.070	0.070	39.2 ± 11.4
12	2.71	25	0.070	0.070	48.5 ± 11.3
13	3.7	25	0.0165	0.070	208 ± 48
14	4.2	25	0.0188	0.068	412 ± 38
15	5.5	25	0.0201	0.051	600 ± 2
16	6.53	25	0.0165	0.070	788 ± 65
17	7.0	25	0.0187	0.068	2620 ± 200
18	7.6	25	0.0165	0.070	7350 ± 400
19	2.0	50	0.0163	0	759 ± 24
20	2	50	0.070	0.070	879 ± 156

[a] A ± value represents one standard deviation of the mean.

The first-order, specific rates of oxygen exchange are given in Table VI as a function of pH and temperature. Because the half-lives for exchange are excessively long at low temperature and pH (e.g., $t_{1/2}$ is 0.76 year at pH 4.3, 0 °C), it was necessary to compute many of the values of k_{obsd} from initial rate measurements, leading to rather large estimated errors. Although the results are not sufficiently precise for detailed mechanistic analysis, the following conclusions and limits can be drawn.

Oxygen exchange with the bulk solvent occurs slowly. From Table VI the rate of the $[H^+]$-independent reaction must be

less than 2.4×10^{-7} s^{-1} at 25 °C and 2.9×10^{-8} s^{-1} at 0 °C. In contrast, oxygen exchange in the complex ion $[Re(en)_2O_2]^{2+}$(aq) has a specific rate of 1.94×10^{-6} s^{-1} at 25 °C.[8] The lower rate for the more highly charged but isoelectronic (d^2) osmium(VI) complex is consistent with a mechanism in which osmium–oxygen bond breakage is the predominant factor in the rate-determining step.

HOCl, which would be expected to oxidize rapidly any $Os(en)_2O_2^+$ present, was found to have little effect on the rate of exchange. Therefore the observed ^{18}O exchange is unlikely to be due to rapid electron exchange between $[Os(en)_2O_2]^{2+}$ and any trace of the possibly labile osmium(V) analogue. Also, the presence of added $en(HCl)_2$ had little effect on the rate of oxygen exchange.

Within the limits of experimental error no appreciable catalysis of ^{18}O exchange by hydrogen ion could be found. In contrast, the rate of oxygen exchange by $[Re(en)_2O_2^+]$ was observed to increase with $[H^+]$ at low pH values.[8] This labilizing effect was ascribed to protonation of oxygen bound to Re(V). We note that the osmyl oxygen ligands in the crystal $[Os(en)_2O_2](HSO_4)_2$ are not formally protonated, although they participate in hydrogen bonding to the hydrogen sulfate ion. Furthermore, the UV–visible spectrum of $[Os(en)_2O_2]^{2+}$(aq) is unchanged in solutions of varying pH ranging from neutral to strongly acidic (1 M H^+). The results indicate a rather low order of basicity for the osmium complex compared with aqueous $Re(en)_2O_2^+$ and $Re(CN)_4O_2^{3-}$ which are protonated at oxygen and which have pK_a of 3.2 and 3.7, respectively.

Lack of an $[H_3O^+]$-dependent path in the oxygen-exchange kinetics of $Os(en)_2O_2^{2+}$ parallels the behavior of the ions $NpO_2(OH_2)_n^{2+}$ and $PuO_2(OH_2)_n^{2+}$. In contrast, $NpO_2(OH_2)_n^+$ shows an important pathway for exchange that is catalyzed by hydrogen ion.[15] It has been demonstrated[15] that both increasing atomic number and oxidation state slow the rate of oxygen exchange in $[MO_2(OH_2)_n]^{n+}$ (U(VI), Np(V), Np(VI), Pu(VI)). In this work we find that either one or both of these factors is operative in the $[M(en)_2O_2]^{n+}$ (Os, Re) case. The magnitude of the effect appears to be much smaller with the transition metal ions. We note, as previously observed in the actinide series,[16] that isoelectronic dioxo ions need show little resemblance in their kinetic behavior for oxygen exchange.

Acknowledgment. We thank the National Science Foundation for support of this work and the University of Missouri for a Summer Faculty Research Fellowship (J.M.M.).

Registry No. $[Os(en)_2O_2](HSO_4)_2$, 61202-83-3; $Os^{18}O_2(en)_2^{2+}$, 61202-84-4.

Supplementary Material Available: Listing of structure factor amplitudes (8 pages). Ordering information is given on any current masthead page.

References and Notes

(1) However, see W. P. Griffith, "The Chemistry of the Rarer Platinum Metals", Interscience, New York, N.Y., 1967, Chapter 3; R. H. Magnuson and H. Taube, *J. Am. Chem. Soc.*, **97**, 5129 (1975).
(2) J. M. Malin and H. Taube, *Inorg. Chem.*, **10**, 2403 (1971).
(3) A. L. Coelho and J. M. Malin, *Inorg. Chim. Acta*, **14**, L41 (1975).
(4) Microanalysis was performed by Galbraith Laboratories, Inc., Knoxville, Tenn.
(5) All calculations were performed on the IBM 370/168 computer system of the University of Missouri. The following programs of other scientists were used: W. C. Hamilton and J. A. Ibers, NUPIK, Picker input program; R. Doedens and J. A. Ibers, NUCLS, least-squares program, a modification of W. Busing and H. Levy's ORFLS program; A. Zalkin, FORDAP, Fourier synthesis program; C. Johnson, ORTEP, thermal ellipsoid plot program; W. C. Hamilton, HORSE, general absorption program; W. C. Hamilton, SORTH, sorting program.
(6) (a) D. T. Cromer and J. T. Waber, *Acta Crystallogr.*, **18**, 104 (1962); (b) D. T. Cromer, *ibid.*, **18**, 17 (1962); (c) J. A. Ibers in "International Tables for X-Ray Crystallography", Vol. 3, Kynoch Press, Birmingham, England, 1962, Table 3.13A; (d) R. F. Stewart, E. R. Davidson, and W. T. Simpson, *J. Chem. Phys.*, **42**, 3175 (1965).
(7) M. Anbar and S. Guttman, *Int. J. Appl. Radiat. Isot.* **4**, 233 (1959).
(8) L. B. Kriege and R. K. Murmann, *J. Am. Chem. Soc.*, **94**, 4557 (1972).
(9) D. W. J. Cruickshank, *Acta Crystallogr.*, **17**, 682 (1964).
(10) G. E. Pringle and T. A. Broadbent, *Acta Crystallogr.*, **19**, 426 (1965).
(11) B. Krebs and K. D. Hasse, *Acta Crystallogr., Sect. B*, **32**, 1334 (1976).
(12) F. H. Kruse, *Acta Crystallogr.*, **14**, 1035 (1961).
(13) L. O. Atovmyan, V. G. Andrianov, and M. A. Porai-Koshits, *Zh. Strukt. Khim.*, **3**, 685 (1962).
(14) F. L. Phillips and A. C. Skapski, *J. Chem. Soc., Dalton Trans.*, 2586 (1975); T. Collin, W. P. Griffith, F. L. Phillips, and A. C. Skapski, *Biochim. Biophys. Acta*, **320**, 745 (1973).
(15) S. W. Rabideau, *J. Phys. Chem.*, **67**, 2655 (1963).
(16) R. K. Murmann and J. C. Sullivan, *Inorg. Chem.*, **6**, 892 (1967).